Recent Advances in Understanding Oxide Traps in pMOS Transistors

T. Grasser[1*], K. Rott[2], H. Reisinger[2], M. Waltl[1], F. Schanovsky[1], W. Goes[1], and B. Kaczer[3]

[1] Institute for Microelectronics, TU Wien, Austria [2] Infineon, Munich, Germany [3] imec, Belgium
[*] Email: grasser@iue.tuwien.ac.at

Abstract

Oxide traps play an important role in the non-ideal behavior of semiconductors and have been suspected to contribute to the bias temperature instability (BTI), hot carrier degradation, random telegraph and $1/f$ noise as well as time-dependent dielectric breakdown. Even though its inadequacy has been repeatedly documented in the literature, charge trapping into these defects is conventionally modeled with extended Shockley-Read-Hall theories. Using the recently suggested time-dependent defect spectroscopy (TDDS), we have demonstrated a number of remarkable features of oxide defects in SiON pMOSFETs, including frequency-dependent capture times, highly bias-sensitive emission times in so-called switching traps as well as temporary random telegraph noise (tRTN). Theoretical modeling of these features requires nonradiative multiphonon theory and the introduction of metastable states.

1. Introduction

The effective capture and emission times of oxide defects have conventionally been studied via the analysis of random telegraph noise (RTN). This method analyzes the fluctuations around the equilibrium occupancy of the traps at a certain bias and works best when capture and emission times are of the same order of magnitude [1–3].

By switching the gate voltage, dynamic transitions between the old and the new equilibrium occupancy can be enforced. This fact has been exploited in the recently introduced time-dependent defect spectroscopy (TDDS) [4], which is a individual-trap variant of the deep-level transient spectroscopy (DLTS) [5,6]. By using constant [7–10] and alternating voltages [11–15] during the charging and discharging phases, these experiments have revealed the following schematic model for the dominant defects in the oxide of SiON pMOSFETs (see Fig. 1): *(i)* Defects can be either fixed positive or switching traps, consistent with previous studies on large-area devices [16–18]. This implies and confirms the existence of a neutral metastable state (1' in our notation). *(ii)* The capture times are strongly bias dependent, consistent with previous RTN studies [1,2] and non-radiative multiphonon (NMP) theory [1,19–21]. However, for very large oxide fields, a saturation behavior is observed. *(iii)* The capture and emission times of individual defects appear de-correlated. This suggests that charging proceeds via a metastable state (2' in our notation).

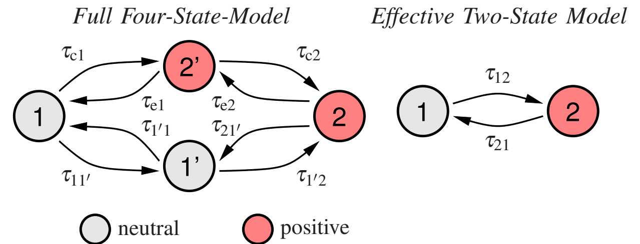

Fig. 1. **Left**: The four states of oxide defects extracted from DC TDDS experiments [4]. Each defect has two stable states, 1 and 2, and possibly two metastable states 1' and 2'. The metastable state 2' seems to be always present, while the existence of the metastable state 1' decides on whether the trap behaves like a fixed positive or a switching trap [16, 17]. **Right**: An effective two-state approximation of the four-state defect using the first-passage times τ_{12} and τ_{21} [4, 22].

Although the assignment of the states shown in Fig. 1 with the various configurations of E' centers [16,17,23] is tempting [4], this issue is still open [24–27].

2. The AC TDDS

In order to confirm the existence of state 2', the DC stress phase of the TDDS setup was replaced by an AC stress [11,15]. Although the two-state approximation is designed to have the same expectation values for the capture and emission times under DC conditions [22], it is fundamentally different under AC conditions because it has a *frequency-independent* effective capture time τ_c [11,28,29]. The full four-state model, on the other hand does result in a *frequency-dependent* effective τ_c [30]. This overall frequency-dependence can be weaker or stronger, depending on the values of the elementary time constants. Since these time constants depend on bias and temperature, the frequency-dependence is also bias and temperature dependent. However, these time constants also describe the DC features of the model, namely the bias and temperature dependence of τ_c and τ_e. As such, if state 2' exists and the model is correct, it must be able to describe τ_c and τ_e under both DC and AC conditions as a function of temperature and bias. In other words, since no new parameters are introduced in the four-state model, both DC and AC conditions must be captured by the same parameter set. Dynamic AC TDDS experiments have confirmed that this is indeed the case [15]. For example, Fig. 2 demonstrates that the defect model accurately captures this frequency-dependence as a function of bias and temperature.

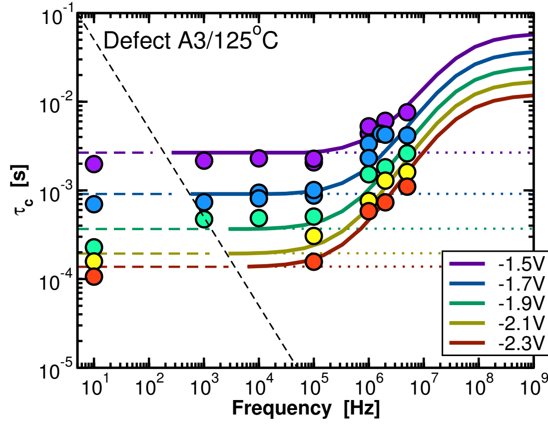

Fig. 2. Comparison of model (lines) and data (symbols) for the bias dependence of τ_c of defect A3 under AC conditions as a function of f at 125 °C. For f larger than a critical frequency f_c about 100 kHz, τ_c increases until it reaches a saturation level. For the conventional first-order (two-state) model, no f dependence is obtained (dotted lines). The dashed lines show the minimum f possible experimentally, given by the requirement that τ_c has to be larger than one half period of the AC signal.

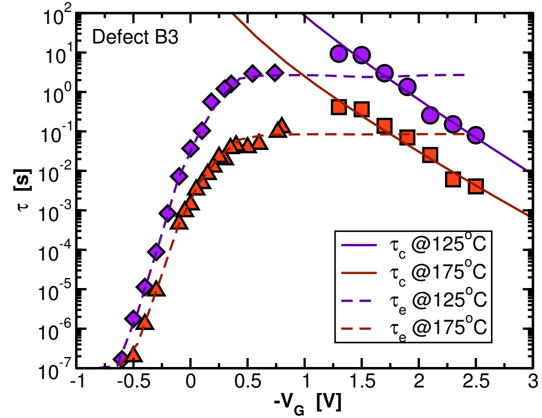

Fig. 3. The capture and emission times of switching trap B3 at two temperatures. The symbols are the data while the lines are from the NMP model. Excellent agreement between theory and data is obtained over 8 orders of magnitude.

3. The Recovery-Pulse TDDS

While charging follows the pathway $1 \rightleftarrows 2' \rightarrow 2$, discharge may proceed either via $2'$ or $1'$. The latter route becomes relevant when the defect level E'_T (the switching level, details in [4]) moves below the Fermi-level of the substrate. Then, the previously charged defect is neutralized ($2 \rightarrow 1'$). The duration of this transition is determined by $\tau_{21'}$, which will have become smaller than the bias-independent $\tau_{22'}$ under these conditions.

Regarding the discharge of the defects it has been observed that some defects, the so-called switching traps, are sensitive to the gate bias [16, 17], while others are not. From a reliability standpoint, it has been demonstrated that the recoverable component of NBTI, which has been linked to such oxide traps [31–38] is highly sensitive to switches into the depletion regime [39–41]. However, the DC TDDS requires a certain current flow through the transistors and τ_e cannot be completely studied in depletion to better understand and link the behavior of individual traps to NBTI. By introducing a well controlled discharge pulse right after stress, we have recently extended the TDDS to allow for the extraction of τ_e throughout the whole depletion and even into the accumulation regimes of the transistor [10], see Fig. 3 for a comparison of model and data for a selected defect.

4. Conclusions

By extending the time-dependent defect spectroscopy (TDDS) to more dynamic cases using AC stresses and controlled pulses right after the charging sequence, the metastable defect states can be probed in a detailed manner. We have summarized some recent results and confirmed the accuracy of the previously suggested multi-state NMP model.

Acknowledgments

The research leading to these results has received funding from the FWF project n°23390-N24 and the European Community's FP7 project n°261868 (MORDRED).

References

[1] A. Palma *et al.*, PRB **56**, 9565 (1997).
[2] N. Zanolla *et al.*, *ULIS* (Udine, Italy, 2008), pp. 137–140.
[3] J. Campbell *et al.*, *IRPS* (2009), pp. 382–388.
[4] T. Grasser *et al.*, *IRPS* (2010), pp. 16–25.
[5] D. Lang, JAP **45**, 3023 (1974).
[6] A. Karwath *et al.*, APL **52**, 634 (1988).
[7] H. Reisinger *et al.*, *IIRW* (2009), pp. 30–35.
[8] H. Reisinger *et al.*, *IRPS* (2010), pp. 7–15.
[9] M. Toledano-Luque *et al.*, JVST B **29**, 01AA04 (2011).
[10] T. Grasser *et al.*, *IRPS* (2013), pp. 2D.2.1–2D.2.7.
[11] M. Toledano-Luque *et al.*, *IRPS* (2011), pp. 364–371.
[12] K. Zhao *et al.*, *IRPS* (2011), pp. 372–380.
[13] J. Zou *et al.*, *SWN* (2012), pp. 1–2.
[14] J. Zou *et al.*, *VLSI Symp.* (2012), pp. 139–140.
[15] T. Grasser *et al.*, *IEDM* (2012), pp. 19.6.1–19.6.4.
[16] A. Lelis *et al.*, T-NS **41**, 1835 (1994).
[17] J. Conley Jr. *et al.*, T-NS **42**, 1744 (1995).
[18] T. Grasser *et al.*, ME **86**, 1876 (2009).
[19] K. Huang *et al.*, Proc.R.Soc.A **204**, 406 (1950).
[20] C. Henry *et al.*, PRB **15**, 989 (1977).
[21] W. Fowler *et al.*, PRB **41**, 8313 (1990).
[22] T. Grasser, *MR* (2012), Vol. 52, pp. 39–70.
[23] E. Poindexter *et al.*, J.Electrochem.Soc. **142**, 2508 (1995).
[24] J. Campbell *et al.*, T-DMR **7**, 540 (2007).
[25] J. Ryan *et al.*, *IRPS* (2010), pp. 43–49.
[26] F. Schanovsky *et al.*, JVST B **29**, 01A2011 (2011).
[27] F. Schanovsky *et al.*, *SISPAD* (2013).
[28] C. Shen *et al.*, APL **86**, 093510 (2005).
[29] H. Reisinger *et al.*, *IRPS* (2011), pp. 597–604.
[30] T. Grasser *et al.*, *IRPS* (2012), pp. XT.8.1–XT.8.7.
[31] V. Huard *et al.*, MR **46**, 1 (2006).
[32] T. Aichinger *et al.*, *IRPS* (2009), pp. 2–7.
[33] V. Huard, *IRPS* (2010), pp. 33–42.
[34] B. Kaczer *et al.*, EDL **31**, 411 (2010).
[35] D. Ang *et al.*, T-DMR **11**, 19 (2011).
[36] Z. Teo *et al.*, *IRPS* (2011), pp. 943–947.
[37] G. Pobegen *et al.*, *IEDM* (2011), pp. 27.3.1–27.3.4.
[38] M. Duan *et al.*, EDL **33**, 480 (2012).
[39] B. Kaczer *et al.*, *IRPS* (2008), pp. 20–27.
[40] T. Aichinger *et al.*, JAP **107**, 024508 (2010).
[41] T. Aichinger *et al.*, APL **96**, 133511 (2010).